7-19-2017

The Solvent- Solid Interface of Acid Catalysts Studied by High Resolution MAS NMR

Robert L. Johnson
Iowa State University

Michael P. Hanrahan
Iowa State University

Max Mellmer
Iowa State University

James A. Dumesic
Iowa State University

Aaron J. Rossini
Iowa State University, arossini@iastate.edu

See next page for additional authors

The Solvent- Solid Interface of Acid Catalysts Studied by High Resolution MAS NMR

Abstract
High-resolution magic angle spinning (HRMAS) NMR spectroscopy was used to study the effect of mixed solvent systems on the acidity at the solid–liquid interface of solid acid catalysts. A method was developed that can exploit benefits of both solution and solid-state NMR (SSNMR) by wetting porous solids with small volumes of liquids (<2>μL/mg) to create an interfacial liquid that exhibits unique motional dynamics intermediate to an isotropic liquid and a rigid solid. Results from these experiments provide information about the influence of the solvent mixtures on the acidic properties at a solid–liquid interface. Importantly, use of MAS led to spectra with full resolution between water in an acidic environment and that of bulk water. Using mixed solvent systems, the chemical shift of water was used to compare the relative acidity as a function of the hydration level of the DMSO-d6 solvent. Nonlinear increasing acidity was observed as the DMSO-d6 became more anhydrous. 1H HR-MAS NMR experiments on a variety of supported sulfonic acid functionalized materials, suggest that the acid strength and number of acid sites correlates to the degree of broadening of the peaks in the 1H NMR spectra. When the amount of liquid added to the solid is increased (corresponding to a thicker liquid layer), fully resolved water phases were observed. This suggests that the acidic proton was localized predominantly within a 2 nm distance from the solid. EXSY 1H–1H 2D experiments of the thin layers were used to determine the rate of proton exchange for different catalytic materials. These results demonstrated the utility of using (SSNMR) on solid–liquid mixtures to selectively probe catalyst surfaces under realistic reaction conditions for condensed phase systems.

Disciplines
Chemical Engineering | Chemistry

Comments
This is manuscript of an article published as Johnson R.L., Hanrahan M.P., Mellmer M., Dumesic J.A., Rossini A.J., Shanks B.H.* The Solvent- Solid Interface of Acid Catalysts Studied by High Resolution MAS NMR, Journal of Physical Chemistry C, 2017, Submitted for Publication.doi: 10.1021/acs.jpcc.7b04102. Posted with permission.

Authors
Robert L. Johnson, Michael P. Hanrahan, Max Mellmer, James A. Dumesic, Aaron J. Rossini, and Brent H. Shanks

The Solvent-Solid Interface of Acid Catalysts Studied by High Resolution MAS NMR

Robert L. Johnson[ab], *Michael P. Hanrahan*[c], *Max Mellmer*[db], *James A. Dumesic*[db], *Aaron J. Rossini*[ce], *Brent H. Shanks.**[ab]

[a]Department of Chemical and Biological Engineering, Ames, IA, 50011

[b]Center for Biorenwable Chemicals (CBiRC) Iowa State University, Ames IA, 50011

[c]Department of Chemistry Iowa State University, Ames IA, 50011

[d]Department of Chemical and Biological Engineering University of Wisconsin, Madison

[e]US DOE Ames Laboratory, Ames, Iowa, USA, 50011

ABSTRACT

High-resolution magic angle spinning (HR-MAS) NMR spectroscopy was used to study the effect of mixed solvent systems on the acidity at the solid-liquid interface of solid acid catalysts. A method was developed that can exploit benefits of both solution and solid-state NMR (SSNMR) by wetting porous solids with small volumes of liquids (< 2 μL/mg) to create an interfacial liquid that exhibits unique motional dynamics intermediate to an isotropic liquid and a rigid solid. Results from these experiments provide information about the influence of the solvent mixtures on the acidic properties at a solid-liquid interface. Importantly, use of MAS led

to spectra with full resolution between water in an acidic environment and that of bulk water. Using mixed solvent systems, the chemical shift of water was used to compare the relative acidity as a function of the hydration level of the d_6-DMSO solvent. Non-linear increasing acidity was observed as the d_6-DMSO became more anhydrous. ^{1}H HR-MAS NMR experiments on a variety of supported sulfonic acid functionalized materials, suggest that the acid strength and number of acid sites correlates to the degree of broadening of the peaks in the ^{1}H NMR spectra. When the amount of liquid added to the solid is increased (corresponding to a thicker liquid layer), fully resolved water phases were observed. This suggests that the acidic proton was localized predominantly within a 2 nm distance from the solid. EXSY ^{1}H-^{1}H 2D experiments of the thin layers were used to determine the rate of proton exchange for different catalytic materials. These results demonstrated the utility of using (SSNMR) on solid-liquid mixtures to selectively probe catalyst surfaces under realistic reaction conditions for condensed phase systems.

1. INTRODUCTION

Conversion of biobased molecules commonly necessitate the reaction to be performed in the condensed phase. A large effect from the solvent has been shown to exist for condensed phase catalysis such as been demonstrated with zeolitic microporous materials.[1-2] The interactions between the solid surface and the solvent introduces a critical parameter that cannot be measured directly with currently available techniques, so information is limited to indirect measurements such as changes in conversion and selectivity. Brønsted acids, which are ubiquitous in biomass conversion and include hydrolysis, dehydration, and esterification reactions, are another catalyst type that is strongly influenced by the solvent system. Previous research on homogeneous

Brønsted acid catalysts for dehydration and hydrolysis reactions has shown that use of polar aprotic solvents led to dramatic increases in reaction rate and selectivity,[3] with up to a 100-fold reaction rate increase. Interestingly, this reaction rate increased non-linearly as the water content was reduced. The observed rate increase was postulated to result from a thermodynamic stabilization of the acidic proton through hydrogen bonding with water, yielding a reduced acidity as the water content was increased. A method to directly measure this effect, such as through the pKa of a strong acid in a mixed solvent, is not readily accessible. Adding to this challenge is the significant environmental and economic incentive to substitute homogeneous acids with heterogeneous acids, such as sulfonated resins, [4] sulfonated carbon materials,[5-8] functionalized silica, [9] and zeolites.[10]

SSNMR has been used extensively to directly characterize the active sites on solid acid surfaces; most commonly these materials have been inorganic solid acids including silica-aluminas, zeolites, and sulfonated zirconias. Direct measurement of ^{27}Al, [11] , ^{17}O [12] and ^{1}H nuclei has been used to measure the acidity of numerous solid acid materials. ^{1}H $\{^{17}$O$\}$ double resonance and ^{1}H $\{^{27}$Al$\}$ double resonance TRAPDOR experiments have been used to probe the proximity of ^{1}H, ^{17}O and ^{27}Al nuclei.[13-14] Although ^{27}Al or ^{1}H SSNMR spectroscopy is an established technique to probe heterogeneous acid material, there are several limitations. First, ^{27}Al SSNMR can only probe acidic sites corresponding to Al species. Furthermore, the structural information that can be obtained is commonly limited since ^{27}Al NMR spectra are often significantly broadened by second-order quadrupolar effects. Direct measurement of the ^{1}H SSNMR spectra can enable acidic protons to be probed. However, the materials must be dry to prevent broadening of signals by exchange with free water. This requires heating above 250 °C in vacuum and will decompose a large number of strong Brønsted acid groups, such as

sulfonated groups, e.g., in Nafion, Amberlyst, and sulfonated carbons. NMR of Lewis base probe molecules bound to acid sites has been used to quantify both the number and strength of acid sites.[15] ^{1}H, ^{2}H, ^{13}C, ^{15}N and ^{31}P SSNMR spectra of probe molecules such as acetone[16-17], methanol[18], pyridinic species,[15,19] and trimethyl phosphine ($P(CH_3)_3$)[19-20] or triethyl phosphine oxide (TEPO) has been demonstrated.[21] Of note is that experiments with TEPO have been validated with comparison to pyridine adsorbtion calorimetry by demonstration of a linear correlation of ^{31}P chemical shifts with pyridine adsorption enthalpy $-\Delta H$ (kcal/mol) .

SSNMR has also been used to characterize the interactions of probe molecules with solid acid sites by observation of in-situ transformations. These measurements were accomplished using a specialized apparatus that could introduce known amounts of gas phase molecules at cryogenic temperatures and has been applied to characterize more than 80 molecules on acidic surfaces via in-situ NMR.[22-23, 24] Further coupling with 2D double quantum magic angle spinning (DQ MAS) homonuclear experiments has been shown to be a powerful technique to probe acidic surfaces and discern reaction mechanisms.[25] While the introduction of gas phase probe molecules onto clean surfaces produces discerning results, the approach still has some limitations. Notably, the approach requires specialized equipment for sample preparation and cannot be used to investigate the role of the solvent in condensed phase systems. Recent work has explored using NMR with zeolite catalyst loaded with small amounts of liquid/reactant mixtures to gain insights about the catalyst reactivity. In zeolites containing small amounts of water different sites on the zeolite catalyst were resolved using a MAS frequency of 5 kHz, and successfully demonstrate that water uptake could be modulated with grafting of hydrophobic residues.[26] Studies have also been used to show the influence of water on C-H bond activation in zeolite catalyst using a similar approach.[27]

Understanding the role of the solvent in condensed phase reactions requires development of methodologies to probe the catalyst surface-liquid interface to elucidate the complex interplay between the solvent, reactant, and surface. NMR of solid-liquid mixtures has been used to reveal information about molecular motions, diffusion, and interactions between phases, as well as being a promising technique for the characterization of functionalized solids dispersed in liquids.[28] These experiments utilized pulse field gradients to measure diffusion rates and molecular interactions through nuclear Overhauser effect (NOESY) experiments. Solid systems with liquid-like components (liquid crystals, gels, and membranes) are particularly interesting, as both liquid and SSNMR can be leveraged. Use of SSNMR to study the liquid-like components of solid-liquid composites, termed high-resolution magic angle spinning (HR-MAS) NMR, has been shown to be a fruitful approach as it leads to NMR spectra with very high resolution compared to NMR spectra of true solid materials. Most often this technique has been applied to biological samples, both swollen and metal supported,[29] functionalized resins and polymers[30-36] such as membranes and biomolecules, linkers on oxide supports,[37] ligands on metal nano-particles,[38] and solid-phase organic reactions;[39] however, this technique is sparsely used to study heterogeneous catalyst surfaces. One example, which utilized this resolution to extract information about interfacial dynamics, was work characterizing water on anion exchange membranes. Using resolved "free water" and protonated water combined with NOESY experiments, the relative rates of exchange between the two phases was compared and provided insight about the rates of crossover between the two domains within the swollen polymeric material.[40]

In the current work, we show how SSNMR spectroscopy can be applied to study porous solids impregnated with thin liquid films. This is a unique approach to examine catalyst surfaces in condensed phase systems. The results are relevant for heterogeneous catalysis under realistic

conditions.[24] This emerging application of HR-MAS NMR has potential to characterize the catalyst-liquid interface and provides information about molecular motions, solid-liquid interactions, and molecular orientations with nanometer resolution, while monitoring reactions in real time.[41-42] We have used this approach to compare a number of solid acid catalysts and investigate the effects of mixed solvent systems on acidity.

2. Experimental Method

2.1 Reagents and Materials

Materials, including D_2O, Davisil silica, propyl-SO_3H silica functionalized silica gel, and trimethoxy propyl sulfide silane, and trimethoxy-ethyl-arene-thiol, were all used as purchased from Sigma. d_6-DMSO was obtained from the Cambridge isotope laboratory and Nafion coated silica (SAC-13-531 13%) from Engelhard. The ZSM-5 zeolite (CBV2314) was purchased from Zeolyst containing a Si:Al of 11.5 and it was calcined at 550 ^oC for 10 hrs to convert the catalyst into to the acidic form. All catalyst materials were degassed in a Micromeretics 2020 BET unit at 105 ^oC for 12 hrs and transferred into the glove box in the sealed BET tube.

2.2 Catalyst preparation

Synthesis of functionalized Davisil silica

The functionalized silica materials were synthesized by adding 10 mmol of propyl or ethyl-arene sulfonic acid methoxysilane to 0.5 grams of Davisil silica to a total volume of 10 ml in dichloromethane in a glove box under a nitrogen atmosphere and held at room temperature for 48 hr. The materials were then washed with 50 ml of dichloromethane, and 30 ml of ethanol under vacuum filtration followed by overnight drying in an oven at 100 ^oC. The materials were then treated with 15 ml of 30% H_2O_2 for 24 hr, followed by filtration and washing with an

additional 100 ml of epure H_2O. To ensure sulfonic acid groups were fully protonated materials were immersed in 30 ml of 1M H_2SO_4 under stiring for 4 hrs. After acidification materials were washed with epure H_2O until the filtrate was no longer strongly acidic and finally were dried at 80 oC in air over night. The total number of acid sites was determined by titration against 0.10 M NaOH using a Titrino-plus auto-titrator.

Preparation of liquid impregnated catalytic materials

2.3 NMR experiments The liquid impregnated catalytic materials used for the NMR analysis were prepared and packed in a glove box. The materials were impregnated by first weighing out approximately 10 mg of the catalyst into a screw cap 2 ml polypropylene tube, followed by application of liquid onto the solid material. The wetted solid was allowed to equilibrate for a minimum of 6 hr (typically overnight). The impregnated materials were then mixed with a spatula, allowed to equilibrate for another 30 minutes, and packed into the 2.5 mm rotors, which were stored in a screw cap vial prior to being analyzed. To ensure that no liquid was being lost during the NMR experiments rotors were weighed before and after NMR experiments and found to contain the same mass.

HRMAS/Solid-State NMR.

^{1}H NMR experiments were acquired with a Bruker Avance III HD solid-state NMR spectrometer with a 9.4 T superconducting magnet (400 MHz ^{1}H Larmor frequency), using a triple resonance 2.5 mm probe. Direct polarization spectra were acquired using power levels corresponding to 90° ^{1}H pulse lengths of 2.5 μs with an acquisition period of 300 ms.

2D EXSY NMR spectra were acquired with a standard three pulse NOESY/EXSY pulse sequence (□/2-t_1-□□/2-□$_{mix}$-□/2). Phase sensitive detection in the indirect dimension was obtained with the STATES-TPPI procedure by cycling the phase of the second 90° degree pulse.

3. RESULTS AND DISCUSSION

3.1 Effect of MAS on peak shape for thin liquid layers

Results comparing the effect of the MAS frequency on the ^{1}H spectra of 5-hydroxymethylfurfural (HMF) and/or H_2O in d_6-DMSO impregnated onto propyl-SO_3H functionalized Davisil silica or ZSM-5, respectively, are shown in Figure 1. These results demonstrated that the thin liquid layer on top of a rigid solid surface could undergo molecular motions that were intermediate to that of a rigid solid or a true isotropic liquid. This is evident from the dramatic effect of MAS, which at even moderate spinning speeds generates high-resolution ^{1}H NMR spectra (peaks with full width half maximum (FWHM) as low as 20 Hz). The effect of MAS frequency on the ^{1}H NMR spectra of HMF impregnated on Davisil silica functionalized with propyl-SO_3H groups (Figure 1a) showed a different response than for acidic water (Figure 1b). The peaks originating from HMF did not have substantially improved resolution with faster MAS, while the water peak at 7.3 ppm, which was in exchange with acid sites, narrowed dramatically as the spinning increased from 6 kHz to 25 kHz. Importantly, no peaks were resolved without MAS, as only a broad signal was observed for HMF (static case). This result was also true for ZSM-5 zeolite impregnated with 0.2% H_2O in d_6-DMSO (Figure 1b). Again, under static conditions only a broad ^{1}H NMR signal was observed, which was centered at the chemical shift for water not undergoing rapid exchange with acidic groups "free water." The signal intensity increased and the peaks sharpened substantially when the MAS

frequency was increased from 6 to 15 kHz, with only a small improvement observed when the MAS frequency increased to 25 kHz. Taken together these experiments suggested that the thin film approach was sufficiently robust to be applied to different materials with both water and organic molecules used as probes.

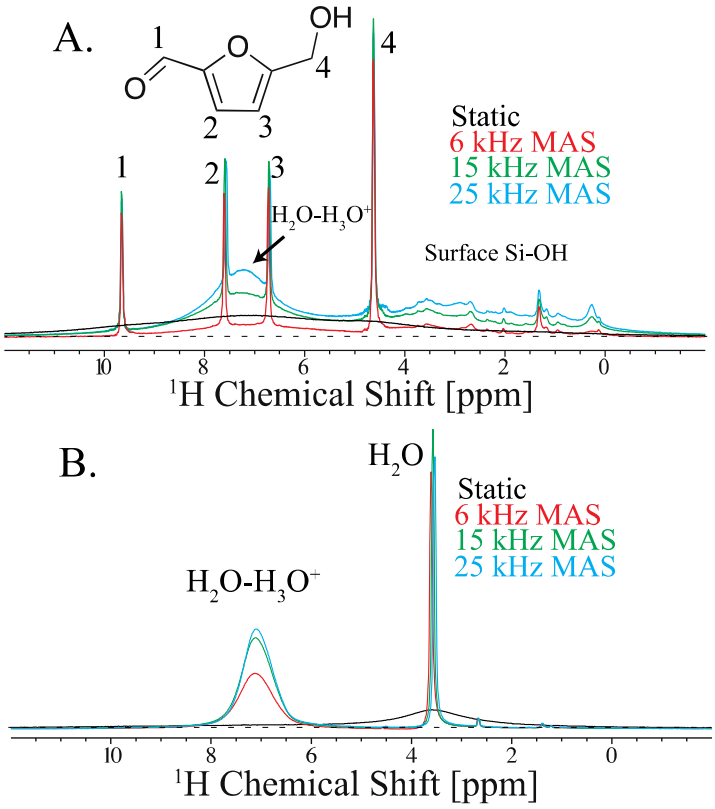

Figure 1. The effect of the MAS frequency of the ^{1}H NMR spectra of thin liquid layers of different solvents impregnated onto solid acid catalysts; (a) 2 M HMF in d_6-DMSO impregnated with 0.66 μL/mg (idealized 2nm liquid layer) onto propyl-SO_3H functionalized silica. ^{1}H NMR spectra obtained with the sample stationary (black trace) and with MAS frequencies of 6 kHz (red), 15 kHz (green) and 25 kHz (blue). (b) Compares ^{1}H NMR spectra of ZSM-5 impregnated with 0.66 μL/mg 0.2% H_2O in d_6-DMSO obtained with the sample stationary (black) and with MAS frequencies of 6 kHz (red), 15 kHz, (green) and 25 kHz (blue).

3.2 Effect of water content on ^1H chemical shift.

The rates of acid-catalyzed dehydration reactions often have pronounced solvent effects.[3, 43] Therefore, experiments were conducted to determine if simple 1D ^{1}H NMR spectra could probe the differences arising from various solvent environments on a Brønsted acid catalyst surface. In highly acidic homogenous solutions the average ^{1}H chemical shift of the water resonance is a convenient measure of the relative acidity because the fast exchange between the acid and water ^{1}H nuclei results in a single resonance reflecting the weighted average of the two independent species.[44] To investigate the relation between water content and acid strength in mixed solvent systems, a set of experiments was conducted in which propyl-SO_3H functionalized silica gel were impregnated with d_6-DMSO containing differing amounts of H_2O/D_2O. The total H_2O content was the same for all samples to keep the signal to noise constant through the series. Spectra from these experiments are shown Figure 2a. The spectra showed a clear trend between decreasing water content and a higher frequency shift accompanied by increased broadening. To more clearly see this correlation, plots were constructed showing the relationship between the peak position and the FWHM (Figure 2b). The plot of peak position vs. FWHM, showed a strong linear relationship. The increase in the ^{1}H chemical shift with the reduction in water concentration in the H_2O/d_6-DMSO solution likely occurs since there is an increase in the relative amount of acid protons with respect to the water protons. Therefore, the average peak position that results from fast exchange between water and acid peaks will shift towards the position of the acid peaks as the concentration of water is reduced. Here we also observe that the degree of broadening is related to the relative concentration of H_3O^+, suggesting that the peak width can provide an additional measure to characterize the acidity of solid acid-solvent interface.

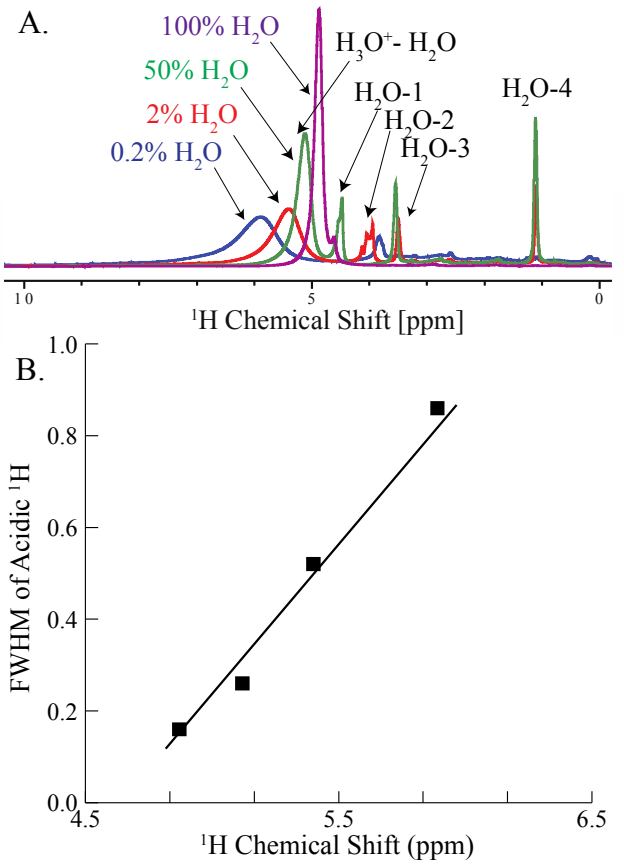

Figure 2. Comparison of water peak ^{1}H chemical shift and FWHM as a function of H_2O content in d_6-DMSO solution for samples of propyl-SO_3H functionalized silica impregnated with 0.66 μL/mg of solid material. This volume to solid ratio was chosen to obtain a theoretical solvent layer thickness of 2 nm in all samples.

3.3 Comparison of H_2O peak position with water content on Davisil and propyl-SO_3H functionalized silica

Samples were prepared to compare how the d_6-DMSO content affected the peak position of the water on the propyl-SO_3H functionalized silica gel versus the non-functionalized silica with similar surface area (Davisil). These samples were used to examine whether the changes in the chemical shift and broadening of the ^{1}H NMR signals of the acid moieties arose from differences

in the water interacting with the acidic surface or greater d_6-DMSO content. Results from this analysis are shown in Figure 3a. The ^{1}H NMR spectra in Figure 3A show the observed H_2O shift to higher ppm ^{1}H NMR signals on propyl-SO_3H functionalized silica was not simply due to changes induced by higher d_6-DMSO content. In fact, as the concentration of d_6-DMSO was increased, the opposite trend was observed. The H_2O ^{1}H NMR signal on un-functionalized Davisil moved to a lower chemical shift with increasing d_6-DMSO content. A plot of the difference in peak position versus d_6-DMSO content is shown in Figure 3b, and it can be seen that the variation in chemical shift with DMSO content is non-linear. Comparatively, a non-linear increasing trend was observed for the monosaccharide dehydration rate (fructose & xylose) and hydrolysis of cellulose glycosidic bonds with decreasing water content in polar aprotic solvents such as DMSO or γ-valerolactone (GVL).[43] Previously, the H_2O ppm shift has been correlated to the wt% H_2SO_4 in H_2O for a homogeneous reaction systems using concentrated sulfuric acid.[45] As the water chemical shift reflects the weighted chemical shifts of all the species in the hydrogen bonding network undergoing fast exchange, the chemical shift of water in a homogeneous solution will be unaffected until high acid concentrations are reached. Given that water under standard condition corresponds to roughly 55 M, a solution of pH 1 is two orders of magnitude lower in concentration and would therefore be unaffected. Using the shift observed for water at the surface of the solid acid catalyst, an estimation of the relative acidity at the surface can be made by correlating to the ^{1}H chemical shift observed for different homogeneous H_2SO_4 concentrations. This analysis shows a non-linear increasing trend which can provide an explanation for increasing reaction rates with decreasing water content in polar aprotic solvents. Using the chemical shifts difference of the concentrated homogeneous acid to determine the effective acid concentration at the surface of the solid catalyst provides a basis to

compare the acidity in these mixed solvent systems. For example, the 2.5 ppm change for the 0.2% water in d_6-DMSO corresponds to roughly the acidity of a 40 wt% sulfuric acid solution, while the modest change of 0.25 ppm in pure water would correspond to a 5 wt% H_2SO_4 solution. Non-linear reaction kinetics was observed and has been proven to follow a specific acid catalyzed kinetic pathway, i.e., kinetic isotope effect k_{D2O}/k_{H2O} >1; H_3O^+ is the catalyst.[46]

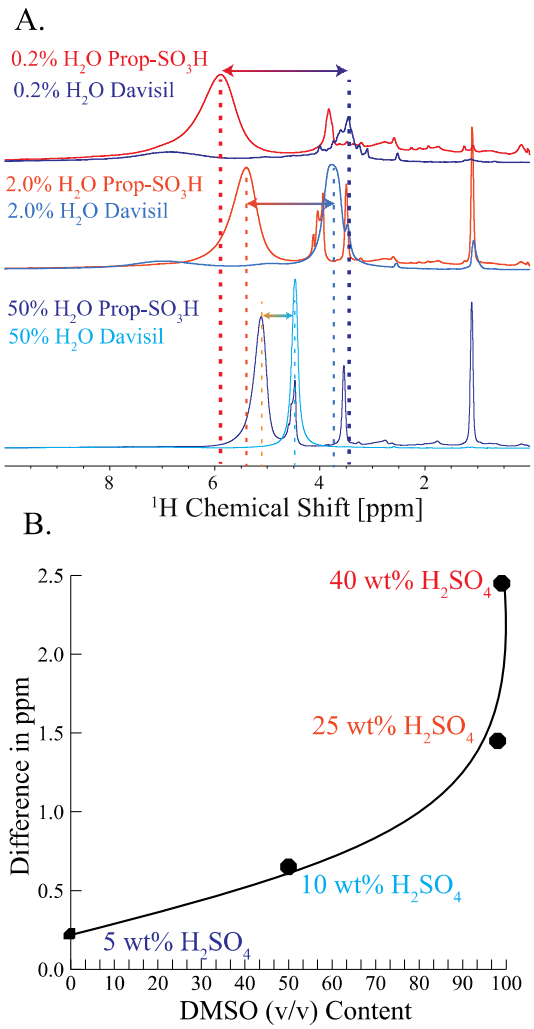

Figure 3. (a) ^{1}H NMR spectra of water-d_6-DMSO solutions impregnated onto Davisil silica or propyl-SO_3H functionalized silica. (b) Plot of the difference in ppm between the Davisil and propyl-SO_3H as a function of DMSO content.

3.4 Effects of total liquid added on ^1H NMR spectra.

To study how the liquid/solid loading, i.e., liquid layer thickness, influenced the ^1H NMR spectra, propyl-SO_3H functionalized silica gel (Sigma) was impregnated with of d_6-DMSO containing 0.2 vol% water and liquid to solid ratios of 0.33, 0.66, or 1.2, μL/mg, to give idealized liquid layers of 1, 2, or 4 nm thickness, respectively. The solid material had an average pore diameter of 7 nm as measured by the BET method, which was used to determine the upper limit of liquid loading that could be used to fill the solid particle pores. Shown in Figure 4a are ^1H NMR spectra that showed two distinct peaks which we assign to "free" (i.e. not in exchange with H_3O^+) water with a chemical shift of ca. 3.66 ppm and acidic water undergoing fast chemical exchange with acidic H_2O, with chemical shifts > 5.5 ppm. The chemical shifts of both acidic H_2O and "free" H_2O remained at nearly the same position at all liquid loadings leading to the important conclusion that the system is not behaving as a homogeneous liquid. The intensity of the "free" water (e.g. 3.66 ppm) signal increases with greater liquid loading in contrast to what is expected in a homogeneous liquid where all of the water molecules in the system would appear at the average signal value reflecting the concentration weighted average of the water ^1H chemical shift and the acid ^1H chemical shift. Therefore, the invariance of the chemical shift of the "free" and acidic H_2O resonances and the variation of their intensities with liquid layer thickness suggests that the "acidic" water signal arises from water in exchange with acid protons that are localized near the surface. Given the estimates of the layer thickness from the volumes of liquid added, this distance can be estimated and these results indicate that the acidic H^+ is localized 1-2 nm near the surface, and represents a means to directly measurement this. Additionally this behavior reflects a micro-environment very close to the solid surface, as the shift to higher ppm with decreasing water content was not simply a result of less total water

available to shift the weighted average towards the position of bulk water. When plotting the area of acidic water and bulk water as a function of liquid loading, a decrease in the relative integrated intensity of the acidic water NMR signal was similar in magnitude to the increase in the integrated intensities of the bulk water NMR signals (Figure 4b). These results indicated that some diffusion across the interface was likely occurring, although on much slower time scales than what can be measured with NMR. Given that the pore diameter was approximately 7 nm, the addition of any more liquid to the system would have exceeded the pore volume and as such the integral of the acidic water would be expected to reach an asymptote. We repeated this experiment with higher H_2O/D_2O concentrations (50%) on the same propyl-SO_3H functionalized silica (Figure S1), and with Nafion coated silica, (Figure S2) and found that the same behavior is observed, ruling out this result being an effect of acid strength or very low water content.

Another difference between the ^1H NMR spectra with different liquid layer thickness was that there are subtle changes in the peak position and shape of the acidic and bulk water peaks with different liquid loadings. With the lowest liquid loading, e.g., corresponding to a 1 nm liquid layer, the acidic peak appeared to be composed of at least two unresolved acidic species. In contrast, the higher loaded samples, having liquid layers of about 2 and 4 nm, gave spectra having only one of the two peaks that were present in the 1 nm case. A possible reason for this behavior was that the 1 nm loading sample had effectively no bulk water present so the liquid film consisted of a layer in which acidic protons exchanged with the entire layer. When the liquid layer was increased to 2 nm only a portion of the acidic water having a NMR signal at lower frequency was present and there was a noticeable amount of bulk water. For the 4 nm layer sample, only the more positively shifted water NMR signal appeared and a larger fraction of bulk water was present. This observation would be consistent with a transition from having a small

layer that could not easily exchange with bulk water to a more clearly defined thicker layer. These results were consistent with previous HR-MAS NMR work that showed clear resolution between surface and bulk water in anion exchange membranes.[40] In that work, pulsed field gradient (PFG) NOESY experiments were also used to determine that exchange between the two phases occurred relatively slowly on the time scale of 50-100 ms. However, given the ambiguity or the pore sizes and concomitant undefined structure of membranes due to swelling/shrinking, a determination of the charge separation distance was difficult.

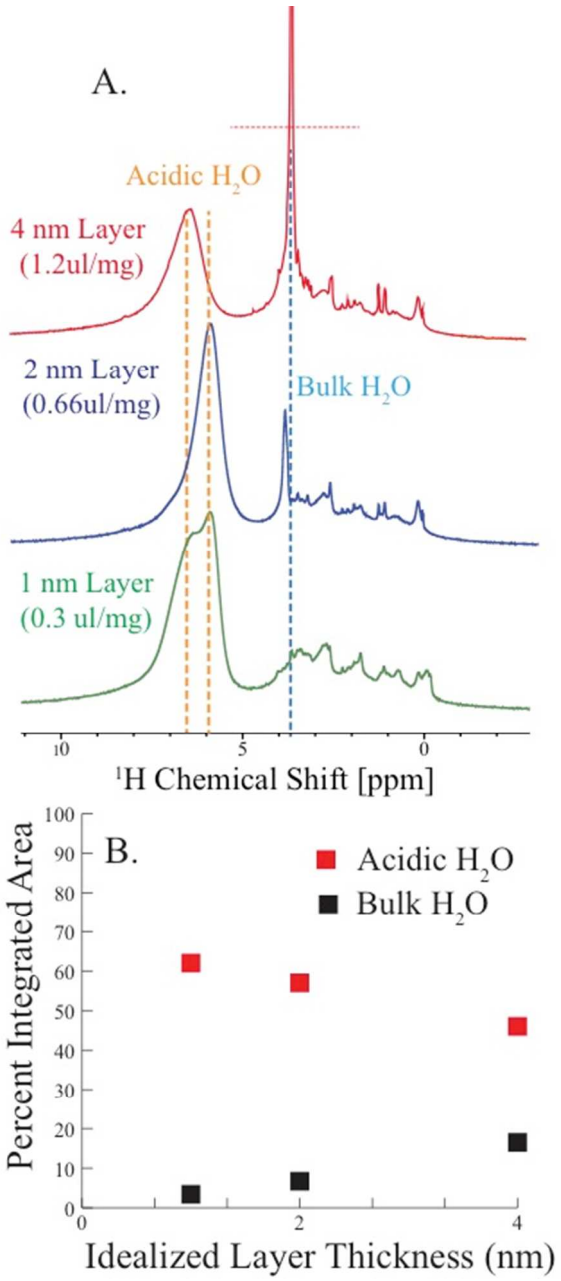

Figure 4. Spectra from 1, 2, 4 nm approximate liquid layers of 0.2% water in DMSO onto propyl-SO_3H functionalized silica gel (a). Plot of integrated intensities for the acidic and bulk water fractions of spectra (b).

3.5 Comparison of different solid acid materials.

An important question in using the ^{1}H chemical shift of the acidic water NMR signal in DMSO solution to probe the acidity of the materials was whether the chemical shift would only reflect the weighted average of the water in exchange with acidic sites or if the peak position would provide information on both the strength of the acid sites *and* the number of sites. This question was examined by comparing four different solid acid materials. Three of the materials had a single well-defined acid group with a known pK_a, and the fourth sample was ZSM-5 zeolite, which is known to contain Brønsted acid sites that do not have readily defined pKa values.[47-48] The spectra resulting from impregnation of these materials with 0.66 μL/mg of 0.2 wt% H_2O in d_6-DMSO are shown in Figure 5. The sample in Figure 5a corresponds to a 13 wt% Nafion polymer supported on an amorphous silica gel, which contained 0.14 mmol of H^+ sites/g and a surface area of 190 m^2/g. The number of acid sites for the functionalized silica materials (Figure 5b and c) as determined by titration was 0.55 mmol/g for the ethyl-arene-SO_3H and 0.45 mmol/g for the propyl-SO_3H, respectively. The first feature of these spectra to note was that the acidic peak had been broadened to a far greater extent for the Nafion material than with the sulfonated silica materials. Secondly, the center of the acidic peak for the Nafion sample was located at a lower ppm value than with the sulfonated silica materials. Further, the broadening decreased with decreasing acid strength of the sulfonated acid groups. For comparison, the spectra is also shown for the impregnated HZSM-5 (Figure 5d).

Interpretation of the NMR results requires consideration of both the number of sites and the acid strength of those sites. The peak position primarily reflects the number of acid sites, as the observed chemical shift is the weighted average of the water chemical shift and the acidic sites. The result of the Nafion material being shifted to lower chemical shift than the functionalized

silica materials would be expected when considering that the number of acid sites is about 4 times less on the Nafion material. Next, a comparison of the arene-SO_3H and propyl-SO_3H peak position showed that the arene-SO_3H (the stronger acid) shifted to a slightly higher ppm than the propyl-SO_3H. Of note, some overlap between the aromatic C-H from the arene-SO_3H and the acidic water did exist that accounted for the sharp spike near 8 ppm. From the chemical shift alone it was difficult to determine if the number of acid sties or the strength of the acid sites led to the arene-SO_3H silica being shifted to a higher ppm value, given these materials do not contain exactly the same number of acid sites.

It is of interest to determine if a spectral feature independent of the number of acid sites could be used to compare acid strengths. When examining the effect of decreasing water in d_6-DMSO the peak was broadened significantly in addition to shifting to a higher ppm. Shown in Figure 5e is a plot of the degree of broadening as measured by the (FWHM) as a function of the pK_a's as determined previously.[49] Comparing Nafion to arene-SO_3H and propyl-SO_3H, a decreasing linear trend was observed with respect to the FWHM of the acidic peak and the pKa of the acid group. With the strongest acid, Nafion, the peaks were broadened to such a large extent that the acidic and bulk water peaks are nearly un-resolved. The increased broadening of the NMR signals observed for the stronger acids has several possible explanations: (i) The weaker acids appear to reside in the slow exchange limit (meaning the exchange rate is slower than the frequency difference) since there are two distinct resonances observed for bulk water and for the acidic water. Stronger acids may have faster exchange rates with bulk water since they are less strongly bound to the conjugate base and there is also a higher concentration of free acid protons. (ii) The free acid protons of stronger acids should have more positive chemical shifts. This will lead to a larger frequency difference between the free acid proton and the water molecules in exchange.

Both (i) and (ii) could result in an intermediate exchange regime where very broad peaks would be observed. If there is a large range of free acid proton chemical shifts then this could lead to broadened peaks, even if exchange between the water and acid protons is fast. When comparing the zeolite to the sulfonated acids, the zeolite material had far greater resolution between the bulk and acidic water peaks, and the acidic peak appeared to be in roughly the same position as the arene-SO_3H functionalized silica, reflecting similar amounts of acid sites. pK_a values obtained for HZSM-5 using Hammet indicators suggested a range of acid sites with pK_a values from -3 to 3 and total acid site amount of 0.5mmol/gram.[47-48] The value obtained from extrapolating the curve led to a pKa value of approximately -1 which was consistent with previous work.

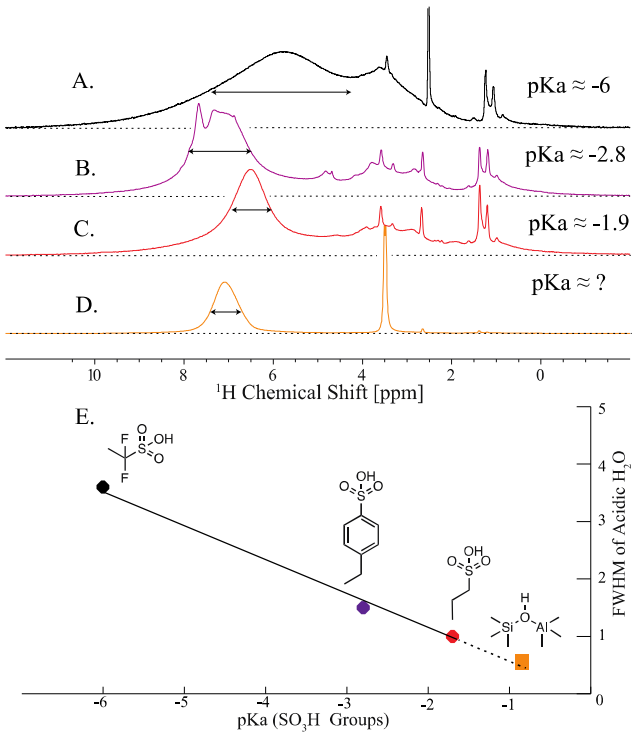

Figure 5. 0.2% H_2O in DMSO impregnated (~2 nm layer) onto; (a) Nafion-coated silica, (b) arene-SO_3H functionalized silica, (c) propyl-SO_3H functionalized silica, (d) HZSM-5 and (e) FWHM versus the known pKa values for the sulfonic acid groups as well as the predicted average pKa acidity of the HZSM-5 from the NMR analysis.

3.6 2D EXSY NMR Experiments on HZSM-5 and propyl-SO_3H functionalized silica

An important difference between zeolites and functionalized silica materials is the large fraction of micropores present in zeolites, which have important implications for catalytic reactivity and selective adsorption of molecules. The Davisil silica used for functionalization contained exclusively mesopores, with an average pore diameter of 14 nm that was dramatically larger than the 0.56 nm pores present in the ZSM-5. This significant difference in pore sizes would be expected to influence the rates of molecular transport, i.e., exchange between the acidic and bulk water impregnated onto the materials surfaces. The exchange behavior was examined using a 2D ^{1}H-^{1}H EXSY experiment comparing the rate of proton exchange between the acidic water and bulk water peaks for the ZSM-5 and propyl-SO_3H functionalized silica (Figure 6). The rate of exchange was found to be much faster for the ZSM-5 material, with a cross-peak intensity already emerging at 10 ms before nearly reaching saturation after 50 ms. In contrast, no significant cross-peak intensity was observed with the propyl-SO_3H functionalized silica, even after 80 ms. The cause of this difference in exchange rates could be due to confinement of the water within the microporous structure, which would likely enhance exchange of protons between the two types of water. Given the larger pores in the mesoporous material, the two types of water could be effectively more separated leading to reduced exchange rates between the two types of water.

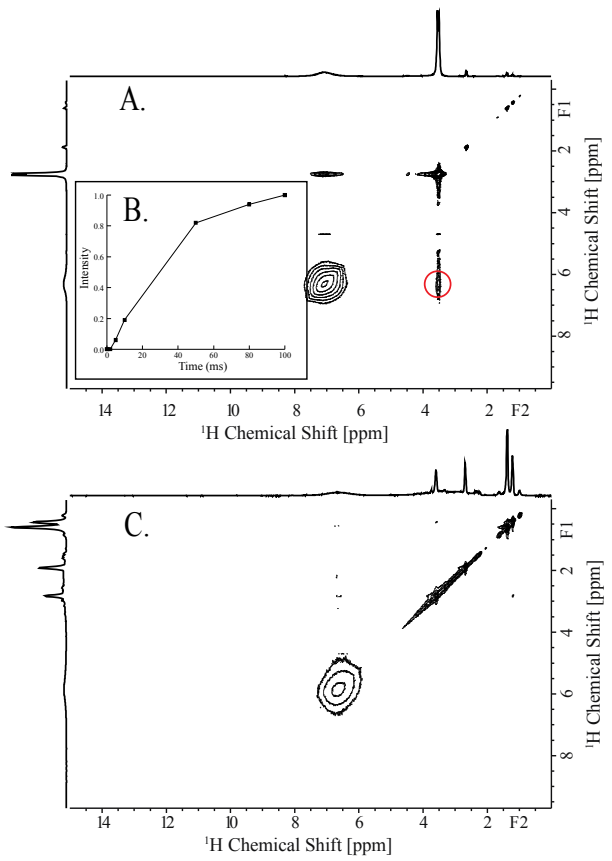

Figure 6. Comparison of 2D EXSY NMR spectra showing exchange between acidic and bulk water in solid acids impregnated with 0.2% H_2O in d_6-DMSO solutions and loading of 0.66 μL/mg. A) 2D EXSY NMR spectrum of ZSM-5 with an 80 ms exchange period, with the inset B) corresponding to intensity buildup from the acidic water to the bulk water due to exchange. Shown in C) is the 80 ms EXSY propyl-SO_3H functionalized silica with the same liquid loading.

4. CONCLUSIONS

Solid acid catalysts were used to demonstrate a unique application of HR-MAS NMR to study heterogeneous catalysts used for condensed phase applications. This was accomplished by impregnating the solid catalysts with a thin liquid layer onto solid surfaces and using the ^{1}H NMR spectra of water in the impregnating liquid as a probe. The molecules of the liquid layer in

contact with the surface display slow motion as evidenced by the dramatic increase in resolution under MAS. High-resolution NMR spectra were obtained that were comparable to what has been acquired with isotropic liquids. To demonstrate the utility of this approach, the effects of water content in polar aprotic solvents on acidity were investigated to understand the origin of the dramatic solvent effects that have been observed for condensed phase acid catalyzed dehydration reactions. The NMR technique showed that as the water content decreased in the solvent, the degree to which the remaining water was acidified increased in an non-linear manner, closely matching previously reported reaction kinetics measurements.

For all of the materials studied it was observed that with increased liquid loading, the NMR spectra revealed two fully resolved NMR signals from the liquid layer. These two signals correspond to water undergoing rapid exchange with the acidic moiety and that of bulk water. From these experiments an estimate of the distance to which the acidic protons were delocalized from the surface was determined by comparing the peak areas for the two resolved species as a function of the nominal thickness of the liquid layer. These results suggested that the solid acid protons were localized predominantly within a 2 nm layer thickness. Moreover, 2D ^{1}H-^{1}H EXSY NMR experiments were used to study the rate of exchange between the acidic water and bulk water for a microporous ZSM-5 and mesoporous propyl-SO_3H functionalized silica. This exchange was found to be much faster in the zeolite than in the mesoporous functionalized silica. This difference likely arises due to confinement effects on condensed phase molecules within micropores compared to liquids within a much larger mesopores. The use of EXSY in these applications could be further expanded to include reactant molecules that could provide a comparative measure of the strength of interactions between a molecule and catalytic active sties.

Lastly, ^{1}H NMR spectra were compared for several solid Brønsted acid catalyst containing groups with known pKa's. ^{1}H NMR spectra using only water as a probe were found to be able to distinguish acids with different strengths via a linear trend between the observed peak width and acid strength. This approach could be applied to study systems such as zeolites that contain Brønsted acids for which measurements of pKa values are difficult to measure.

The NMR experiments demonstrated on these systems were straightforward, did not require isotopic enrichment, and could be applied with minimal spectroscopic expertise. Therefore, they have the potential to be broadly applied as a novel tool for characterizing catalysts in condensed phase applications. Coupling this approach with the use of ^{13}C enrichment, the scope of systems that could be experimentally interrogated could be expanded. We anticipate that HR-MAS NMR should be applicable to probe impregnated heterogenous catalysts such as metal nanoparticles, acids, and bases. The techniques should allow the directly investigation of numerous questions that persist in the field of condensed phase heterogeneous catalysis, including solvent effects, support effects, mechanistic studies, catalyst deactivation, and provide support to quantum chemical modeling of heterogenous catalysts.

ASSOCIATED CONTENT

Supporting Information. This material is available free of charge on the ACS publication website at DOI: http://pubs.acs.org.

^{1}H NMR spectra with 50% H_2O in d_6-DMSO with 1, 2, 4 nm layer thickness, 1, 2, 4 nm loadings of 0.2% H_2O in d_6-DMSO loading onto Nafion coated silica, spectra of ethyl-arene sulfonate before and after neutralization with NaOH, ammonia TPD of CBV2314 ZSM5 zeolite, CBV2314 with 100% *d6*-DMSO.

AUTHOR INFORMATION

Corresponding Author
*E-mail: bshanks@iastate.edu

ORCID
Brent H. Shanks:

Notes
The authors declare no competing financial interests

ACKNOWLEDGMENT

This work was supported in part by the NSF Engineering Research Center for Biorenewable Chemicals (CBiRC), and award number EEC-0813570 and the DOE Great lakes Bioenergy Research center (GLBRC). We thank the Ames Laboratory for use of NMR probes and rotors, and lastly Grace Cattrell for valuable contributions to illustrations.

REFERENCES

1. Derouane, E. G., Zeolites As Solid Solvents. *J. Mol. Catal. A: Chem.* **1998**, *134*, 29-45.
2. Saravanamurugan, S.; Palanichamy, M.; Arabindoo, B.; Murugesan, V., Liquid Phase Reaction Of 2′-Hydroxyacetophenone And Benzaldehyde Over Zsm-5 Catalysts. *J. Mol. Catal. A: Chem.* **2004**, *218*, 101-106.
3. Mellmer, M. A.; Sener, C.; Gallo, J. M. R.; Luterbacher, J. S.; Alonso, D. M.; Dumesic, J. A., Solvent Effects In Acid-Catalyzed Biomass Conversion Reactions. *Angew. Chem. Int. Ed.* **2014**, *53*, 1521-3773.
4. Zhang, X.; Zhao, Y.; Xu, S.; Yang, Y.; Liu, J.; Wei, Y.; Yang, Q., Polystyrene Sulphonic Acid Resins with Enhanced Acid Strength Via Macromolecular Self-Assembly Within Confined Nanospace. *Nat Commun* **2014**, *5*.
5. Anderson, J. M.; Johnson, R. L.; Schmidt-Rohr, K.; Shanks, B. H., Solid State NMR Study Of Chemical Structure and Hydrothermal Deactivation Of Moderate-Temperature Carbon Materials With Acidic SO_3H Sites. *Carbon* **2014**, *74*, 333-345.
6. Antunes, M. M.; Russo, P. A.; Wiper, P. V.; Veiga, J. M.; Pillinger, M.; Mafra, L.; Evtuguin, D. V.; Pinna, N.; Valente, A. A., Sulfonated Graphene Oxide As Effective Catalyst For Conversion Of 5-(Hydroxymethyl)-2-Furfural Into Biofuels. *ChemSusChem* **2014**, *7*, 804-812.

7. Liu, F.; Sun, J.; Zhu, L.; Meng, X.; Qi, C.; Xiao, F.-S., Sulfated Graphene As An Efficient Solid Catalyst For Acid-Catalyzed Liquid Reactions. *J. Mater. Chem.* **2012**, *22*, 5495-5502.

8. Oliveira, B. L.; Teixeira da Silva, V., Sulfonated Carbon Nanotubes As Catalysts For The Conversion Of Levulinic Acid Into Ethyl Levulinate. *Catal. Today* **2014**, *234*, 257-263.

9. Tucker, M. H.; Crisci, A. J.; Wigington, B. N.; Phadke, N.; Alamillo, R.; Zhang, J.; Scott, S. L.; Dumesic, J. A., Acid-Functionalized SBA-15-Type Periodic Mesoporous Organosilicas And Their Use In The Continuous Production of 5-Hydroxymethylfurfural. *ACS Catal.* **2012**, *2*, 1865-1876.

10. Taarning, E.; Osmundsen, C. M.; Yang, X.; Voss, B.; Andersen, S. I.; Christensen, C. H., Zeolite-Catalyzed Biomass Conversion To Fuels and Chemicals. *Energy Environ. Sci.* **2011**, *4*, 793-804.

11. Mardkhe, M. K.; Keyvanloo, K.; Bartholomew, C. H.; Hecker, W. C.; Alam, T. M.; Woodfield, B. F., Acid Site Properties Of Thermally Stable, Silica-Doped Alumina As A Function Of Silica/Alumina Ratio And Calcination Temperature. *Appl. Catal., A* **2014**, *482*, 16-23.

12. Peng, L.; Liu, Y.; Kim, N.; Readman, J. E.; Grey, C. P., Detection Of Bronsted Acid Sites In Zeolite HY With High-Field ^{17}O-MAS-NMR Techniques. *Nat Mater* **2005**, *4*, 216-219.

13. Crépeau, G.; Montouillout, V.; Vimont, A.; Mariey, L.; Cseri, T.; Maugé, F., Nature, Structure And Strength Of The Acidic Sites Of Amorphous Silica Alumina: An IR And NMR Study. *J. Phys. Chem. B* **2006**, *110*, 15172-15185.

14. Gabrienko, A. A.; Danilova, I. G.; Arzumanov, S. S.; Toktarev, A. V.; Freude, D.; Stepanov, A. G., Strong Acidity Of Silanol Groups Of Zeolite Beta: Evidence From The Studies By IR Spectroscopy Of Adsorbed CO And ^{1}H MAS NMR. *Microporous Mesoporous Mater.* **2010**, *131*, 210-216.

15. Liang, S. H. C.; Gay, I. D., Measurement Of Surface Acid Site Concentration By Carbon-13 NMR. *J. Catal.* **1980**, *66*, 294-300.

16. Barich, D. H.; Nicholas, J. B.; Xu, T.; Haw, J. F., Theoretical And Experimental Study Of the ^{13}C Chemical Shift Tensors of Acetone Complexed With Brønsted And Lewis Acids. *J. Am. Chem. Soc.* **1998**, *120*, 12342-12350.

17. Fang, H.; Zheng, A.; Chu, Y.; Deng, F., ^{13}C Chemical Shift Of Adsorbed Acetone For Measuring The Acid Strength Of Solid Acids: A Theoretical Calculation Study. *J. Phys. Chem. C.* **2010**, *114*, 12711-12718.

18. Thursfield, A.; Anderson, M. W., H, ^{2}H, and ^{13}C Solid-State NMR Studies Of Methanol Adsorbed On A Series Of Acidic Microporous Zeotype Materials. *J. Phys. Chem.* **1996**, *100*, 6698-6707.

19. Haw, J. F.; Zhang, J.; Shimizu, K.; Venkatraman, T. N.; Luigi, D.-P.; Song, W.; Barich, D. H.; Nicholas, J. B., NMR And Theoretical Study Of Acidity Probes On Sulfated Zirconia Catalysts. *J. Am. Chem. Soc.* **2000**, *122*, 12561-12570.

20. Ehresmann, J. O.; Wang, W.; Herreros, B.; Luigi, D.-P.; Venkatraman, T. N.; Song, W.; Nicholas, J. B.; Haw, J. F., Theoretical And Experimental Investigation of the Effect Of Proton Transfer On The ^{27}Al MAS NMR Line Shapes Of Zeolite−Adsorbate Complexes: An Independent Measure Of Solid Acid Strength. *J. Am. Chem. Soc.* **2002**, *124*, 10868-10874.

21. Osegovic, J. P.; Drago, R. S., Measurement Of The Global Acidity Of Solid Acids By ^{31}P MAS NMR Of Chemisorbed Triethylphosphine Oxide. *J. Phys. Chem. B.* **2000**, *104*, 147-154.

22. Xu, T.; Munson, E. J.; Haw, J. F., Toward A Systematic Chemistry Of Organic Reactions In Zeolites: In Situ NMR Studies Of Ketones. *J. Am. Chem. Soc.* **1994**, *116*, 1962-1972.

23. Xu, T.; Zhang, J.; Haw, J. F., Imine Chemistry In Zeolites: Observation Of Gem-Amino-Hydroxy Intermediates By In Situ ^{13}C And ^{15}N NMR. *J. Am. Chem. Soc.* **1995**, *117*, 3171-3178.

24. Haw, J. F.; Nicholas, J. B.; Xu, T.; Beck, L. W.; Ferguson, D. B., Physical Organic Chemistry Of Solid Acids: Lessons From In Situ NMR And Theoretical Chemistry. *Acc. Chem. Res.* **1996**, *29*, 259-267.

25. Zheng, A.; Li, S.; Liu, S.-B.; Deng, F., Acidic Properties And Structure–Activity Correlations Of Solid Acid Catalysts Revealed By Solid-State NMR Spectroscopy. *Acc. Chem. Res.* **2016**, *49*, 655-663.

26. Chen, K.; Kelsey, J.; White, J. L.; Zhang, L.; Resasco, D., Water Interactions In Zeolite Catalysts And Their Hydrophobically Modified Analogues. *ACS Catal.* **2015**, *5*, 7480-7487.

27. Chen, K.; Damron, J.; Pearson, C.; Resasco, D.; Zhang, L.; White, J. L., Zeolite Catalysis: Water Can Dramatically Increase Or Suppress Alkane C–H Bond Activation. *ACS Catal.* **2014**, *4*, 3039-3044.

28. Lehman, S. E.; Tataurova, Y.; Mueller, P. S.; Mariappan, S. V. S.; Larsen, S. C., Ligand Characterization Of Covalently Functionalized Mesoporous Silica Nanoparticles: An NMR Toolbox Approach. *J. Phys. Chem. C.* **2014**, *118*, 29943-29951.

29. Favier, I.; Gómez, M.; Muller, G.; Picurelli, D.; Nowicki, A.; Roucoux, A.; Bou, J., Synthesis Of New Functionalized Polymers And Their Use As Stabilizers Of Pd, Pt, And Rh Nanoparticles. Preliminary Catalytic Studies. *J. Appl. Polym. Sci.* **2007**, *105*, 2772-2782.

30. Ruhland, T.; Andersen, K.; Pedersen, H., Selenium-Linking Strategy For Traceless Solid-Phase Synthesis: Direct Loading, Aliphatic C−H Bond Formation Upon Cleavage And Reaction Monitoring By Gradient MAS NMR Spectroscopy. *J. Org. Chem.* **1998**, *63*, 9204-9211.

31. Martins, J. C.; Mercier, F. A. G.; Vandervelden, A.; Biesemans, M.; Wieruszeski, J.-M.; Humpfer, E.; Willem, R.; Lippens, G., Fine-Tuned Characterization At The Solid/Solution Interface Of Organotin Compounds Grafted Onto Cross-Linked Polystyrene By Using High-Resolution MAS NMR Spectroscopy. *Chem. Eur. J.* **2002**, *8*, 3431-3441.

32. Pinoie, V.; Poelmans, K.; Miltner, H. E.; Verbruggen, I.; Biesemans, M.; Assche, G. V.; Van Mele, B.; Martins, J. C.; Willem, R., A Polystyrene-Supported Tin Trichloride Catalyst With A C11-Spacer. Catalysis Monitoring Using High-Resolution Magic Angle Spinning NMR. *Organometallics* **2007**, *26*, 6718-6725.

33. Melchels, F. P. W.; Velders, A. H.; Feijen, J.; Grijpma, D. W., Photo-Cross-Linked Poly(Dl-Lactide)-Based Networks. Structural Characterization By HR-MAS NMR Spectroscopy And Hydrolytic Degradation Behavior. *Macromolecules.* **2010**, *43*, 8570-8579.

34. Brulé, E.; de Miguel, Y. R.; Hii, K. K., Chemoselective Epoxidation Of Dienes Using Polymer-Supported Manganese Porphyrin Catalysts. *Tetrahedron.* **2004**, *60*, 5913-5918.

35. Melean, L. G.; Haase, W.-C.; Seeberger, P. H., A Novel 4,5-Dibromooctane-1,8-Diol Linker For Solid-Phase Oligosaccharide Synthesis. *Tetrahedron Lett.* **2000**, *41*, 4329-4333.

36. Poelmans, K.; Pinoie, V.; Verbruggen, I.; Biesemans, M.; Van Assche, G.; Deshayes, G.; Degée, P.; Dubois, P.; Willem, R., Catalytic Properties Of Cross-Linked Polystyrene Grafted Diorganotins In A Model Transesterification And The Ring-Opening Polymerization Of E-Caprolactone. *Appl. Organomet. Chem.* **2007**, *21*, 504-513.

37. Blümel, J., Linkers And Catalysts Immobilized On Oxide Supports: New Insights By Solid-State NMR Spectroscopy. *Coord. Chem. Rev.* **2008**, *252*, 2410-2423.

38. Zhou, H.; Du, F.; Li, X.; Zhang, B.; Li, W.; Yan, B., Characterization Of Organic Molecules Attached To Gold Nanoparticle Surface Using High Resolution Magic Angle Spinning ^{1}H Nmr. *J. Phys. Chem. C.* **2008**, *112*, 19360-19366.

39. Rousselot-Pailley, P.; Ede, N. J.; Lippens, G., Monitoring Of Solid-Phase Organic Synthesis On Macroscopic Supports By High-Resolution Magic Angle Spinning NMR. *J. Comb. Chem.* **2001**, *3*, 559-563.

40. Jenkins, J. E.; Hibbs, M. R.; Alam, T. M., Identification Of Multiple Diffusion Rates In Mixed Solvent Anion Exchange Membranes Using High Resolution MAS NMR. *ACS Macro Lett.* **2012**, *1*, 910-914.

41. Roy, A. D.; Jayalakshmi, K.; Dasgupta, S.; Roy, R.; Mukhopadhyay, B., Real Time HR–MAS NMR: Application In Reaction Optimization, Mechanism Elucidation And Kinetic Analysis For Heterogeneous Reagent Catalyzed Small Molecule Chemistry. *Magn. Reson. Chem.* **2008**, *46*, 1119-1126.

42. Warrass, R.; Lippens, G., Quantitative Monitoring Of Solid Phase Organic Reactions By High-Resolution Magic Angle Spinning NMR Spectroscopy. *J. Org. Chem.* **2000**, *65*, 2946-2950.

43. Mellmer, M. A.; Martin Alonso, D.; Luterbacher, J. S.; Gallo, J. M. R.; Dumesic, J. A., Effects Of [Gamma]-Valerolactone In Hydrolysis Of Lignocellulosic Biomass To Monosaccharides. *Green Chem.* **2014**, *16*, 4659-4662.

44. Fukuhara, K.; Nakajima, K.; Kitano, M.; Kato, H.; Hayashi, S.; Hara, M., Structure And Catalysis Of Cellulose-Derived Amorphous Carbon Bearing SO_3H Groups. *ChemSusChem.* **2011**, *4*, 778-784.

45. Giammatteo, J. E. a. P., On-Line Acid Strength And Sulfuric Acid Alkylation Process Control Using Process NMR. *Power Point Presentation, Process NMR Associates, LLC* **1998**, *Danbury Ct*.

46. Cordes, E. H.; Bull, H. G., Mechanism And Catalysis For Hydrolysis Of Acetals, Ketals, And Ortho Esters. *Chem. Rev.* **1974**, *74*, 581-603.

47. Wang, K.; Wang, X.; Li, G., Quantitatively Study Acid Strength Distribution On Nanoscale ZSM-5. *Microporous Mesoporous Mater.* **2006**, *94*, 325-329.

48. Sannino, F.; Pansini, M.; Marocco, A.; Bonelli, B.; Garrone, E.; Esposito, S., The Role Of Outer Surface/Inner Bulk Bronsted Acidic Sites in the Adsorption Of A Large Basic Molecule (Simazine) on H-Y Zeolite. *PCCP.* **2015**, *17*, 28950-28957.

49. Guthrie, J. P., Hydrolysis Of Esters Of Oxy Acids: pka Values For Strong Acids; Brønsted Relationship For Attack Of Water At Methyl; Free Energies Of Hydrolysis Of Esters Of Oxy Acids; And A Linear Relationship Between Free Energy Of Hydrolysis And pka Holding Over A Range Of 20 pka Units. *Can. J. Chem.* **1978**, *56*, 2342-2

TOC Graphic

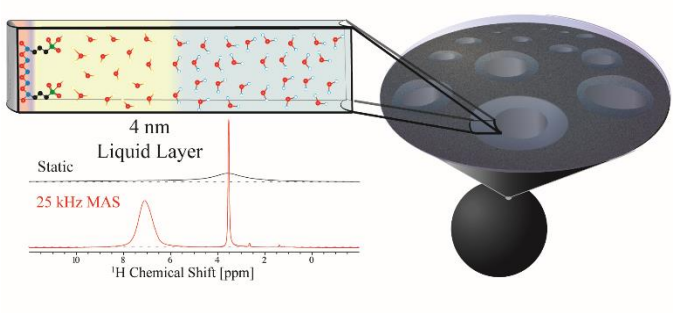
4 nm
Liquid Layer
Static
25 kHz MAS
10
8
6
4
2
0
¹H Chemical Shift [ppm]